Iraqi Journal of Physics, 2025 *Vol.23, No.1, PP. 45-55*
https://doi.org/10.30723/ijp.v23i1.1306
P-ISSN: 2070-4003
E-ISSN: 2664-5548

Analysis of Aloe Vera Plasma Parameters Using Optical Emission Spectroscopy

Weam Aqeel Kazim[1a*] and Alyaa Hussein Ali[1b]
[1]*Department of Physics, College of Sciences for Women, University of Baghdad, Iraq*
[a*]Corresponding author: alyaaha_phys@csw.uobaghdad.edu.iq

Abstract
Optical emission spectroscopy (OES) is used to analyse the main properties of Aloe Vera plasma, where the plasma is generated using a plasma jet. Several parameters of the plasma are measured, including electron temperature (T_e), electron density (n_e), plasma frequency (f_p), Debye length (λ_D), and Debye number (N_D). The study is based on the use of different laser energies ranging from 100 to 400 mJ. The Boltzmann scheme was applied to evaluate the electron temperature, which is based on the analysis of the spectral intensity of optical emissions from the plasma. Stark line broadening was used to figure out the electron density. This method shows how the electric fields created by electrons in the plasma change the width of the spectral lines. In this experiment, the target (Aloe Vera material) was exposed to the laser from a distance of 8 cm. In comparison, the emitted radiation was measured using an optical fiber at a distance of 0.5 cm from the target. All measurements were performed in air, where the electron temperature ranged between 0.793 and 1.124 eV. The results indicated that the electron temperature and density increased with increasing laser power. This increase is in line with expectations, as higher laser power leads to greater detuning of matter and an increase in the number of electrons generated in the plasma, which increases the plasma density and temperature.

Article Info.

Keywords:
Boltzmann Plot, Stark's Line Broadening, Laser Induced Breakdown Spectroscopy (LIBS), Optical emission spectroscopy (OES), Aloe Vera.

Article history:
Received: May,29,2024
Revised: Oct. 03, 2024
Accepted: Oct. 29, 2024
Published:Mar.01,2025

1. Introduction

Aloe vera contains a wide range of biologically active compounds such as sugars, vitamins, amino acids, minerals, and enzymes. When exposed to plasma, specific chemical reactions may occur with these compounds, improving their properties or changing them to be more effective in specific applications such as medical treatments. Aloe Vera plasma can enhance the antibacterial and anti-inflammatory properties already present in Aloe Vera. Optical emission spectroscopy is a branch of spectroscopy that studies the light emitted by a substance when exposed to energy. This energy can be heat, electricity, or other energy, which excites atoms or molecules within the substance. When these atoms or molecules return to their ground state, they release the acquired energy in the form of light. This light has specific wavelengths associated with the chemical elements that make up the substance. Optical emission spectroscopy analyzes this emitted light to distinguish its wavelengths, which helps in identifying the elements present in a sample. Each chemical element has a unique spectrum represented by a series of distinct lines in the emitted spectrum. By studying these lines, scientists can identify and determine the concentrations of different elements in a substance. Optical emission spectroscopy is widely used in many fields, such as physics, chemistry, and medicine, where it is used to analyze different materials and identify their composition. The optical emission spectrum is a powerful and precise tool that allows to understand the properties of matter at the atomic and molecular level, which helps in wide range of scientific and technical applications. The Laser-Induced Breakdown Spectroscopy (LIBS) approach's straight forward characteristics make it a potentially expanding applicable techniques in elemental analysis [1]. This is a potential analytical method for detecting solid, liquid, and gaseous materials. The technique relies on the optical detection of particular atomic and molecular species by observing the emission signals they produce in the plasma generated by a laser [2]. Atoms, ions, and electrons are the principal components of plasma and offer a complete picture of the elements that comprise the basic structure [3, 4]. Plasma diagnostics can be carried out with electron density (n_e) and plasma temperature (T_e) measurements. The total electron density of the plasma shows its thermodynamic equilibrium state. The plasma temperature has a direct impact on the amplitude of various distribution functions that characterize the plasma's state [5, 6]. Due to its dependability, ease of use, speed, and accurate in situ chemical analysis with acceptable detection limits and cost, LIBS can be regarded as a technique appropriate for a broad range of diverse applications [7, 8]. This work examines a diagnostic of a fundamental wavelength of Aloe Vera plasma in air, which caused the sample to evaporate and ionize in the plasma. The sample is then evaluated later by a spectrometer to determine which components are distinct in terms of spectrum. Using the spectral lines released by the Aloe Vera -plasma in air, the spectroscopic studies result of the electron density and plasma temperature were determined. Using plasma spectra, these chemical changes can be precisely determined, providing a deeper understanding of how natural materials interact with plasma. Aloe Vera contains complex sugars, polyphenols, and other biologically active substances that can interact in unique ways with plasma. Studying the light emission spectrum of these interactions may reveal new interactions or produce unexpected materials with new applications that have not been studied with other materials. This paper analyzes the properties of Aloe Vera plasma using optical emission spectroscopy (OES). Aloe Vera plasma is an important biomaterial due to its wide applications in medicine. OES allows a detailed study of the plasma composition by analyzing the light emissions produced by ionization. Through this analysis, one can accurately identify the chemical elements present and understand their behavior within the plasma, which contributes to improve the uses of Aloe Vera and develop new applications. This study looks at a diagnostic of the Aloe Vera plasma's basic wavelength in air. The sample is then evaluated later by a spectrometer to determine which components are distinct in terms of spectrum. Using the spectral lines released by the Aloe Vera plasma in air, spectroscopic studies of the electron density and plasma temperature were obtained. The first step in the visual absorption process is sampling LIBS, which enables the study of solids, liquids, and gases.

2. Theory

The first step in the visual absorption process is sampling LIBS, which enables the study of solids, liquids, and gases [9, 10]. A spectrometer and detector are used to detect plasma light produced when the sample material is ionized and ablates by the laser pulse's intensity [11, 12]. Emission line properties, such as breadth, forms, and shifts, can be used to extract information, including temperature and electron density, from the resulting plasma spectrum [13, 14]. The search was conducted using the Boltzmann plot approach; the measured temperature of the generated plasma is an important characteristic because it may be used to characterize the properties of the plasma. The Boltzmann plot method is widely used in LIBS studies to report plasma temperatures. This method is mainly used in the analysis of atomic and electronic spectra to measure the temperatures of plasma systems (such as thermal plasma). The basic idea behind this method is based on the Boltzmann distribution, which describes the distribution of particles (such as atoms or ions) at different energy levels in a thermal system at equilibrium. Steps for applying the Boltzmann method: collection of spectral data to measure the intensity of the spectral lines for several transitions between different energy levels in the atoms or ions within the sample; for each spectral line, the energy levels of the transition in question are determined, and this information can be obtained from spectral tables or databases; The Boltzmann equation is applied, which relates the intensity of the spectral line (I) to the number of atoms in a given energy level and the temperature.

The average plasma temperature is represented by the temperature (T) as determined by this technique. Eq. (1) is utilized [15, 16]:

$$T = \frac{(E_2 - E_1)}{k \ln(\frac{I_1 \lambda_1 A_2 g_2}{I_2 \lambda_2 A_1 g_1})} \quad (1)$$

where: I is the intensity of the spectral lines, g is the weight (statistical), A is the transformation probability, λ is wavelength, E is the excited state energy, K is Boltzmann constant.

In the further stages of spectral line ionization, Saha-Boltzmann equation is employed. It is given as [15]:

$$n_e = \frac{I_1}{I_2^*} \, 6.04 \times 10^{21} \, (10)^{\frac{3}{2}} \; e^{\frac{(E_1 - E_2 - X_z)}{KT}} \quad cm^{-3} \quad (2)$$

where:

$$I_2^* = \frac{I_2 \lambda_2}{g_2 \, A_2} \quad (3)$$

where: X_z represents the organism's ionization potential at the second ionization level, measured in electron volts (eV). The intensity of the line for the transition from the highest level 2 to level 1 is represented by I_2. The wavelength of the transition from level 2 to level 1 that is considered acceptable is represented by the symbol λ. g_2 is the statistical weight of the transition from level 2 to level 1, A_2 is the probability changes, and the mentioned types' ionization stage is indicated by the z [17-19]. Although the frequency of plasma generated can be determined using the equation [14]:

$$f_p = 8.98 \sqrt{n_e} \quad HZ \quad (4)$$

One fundamental characteristic of plasmas is their frequency, which is solely dependent on their density. Normally, small n_e leads to a very high plasma frequency [20-22].

The quasi-neutrality of plasma is ascribed to Debye shielding (λ_D), wherein charged particles respond to mitigate the influence of adjacent electrical fields. The distance λ_D specifies the Debye length [23, 24]:

$$\lambda_D = \sqrt{\frac{\epsilon_\circ K_B T_e}{e^2 n_e}} = 7.43 \times 10^2 \sqrt{\frac{T_e}{n_e}} \quad (5)$$

where N_D represents the particle density on the Debye surface based on the density and electron's temperature. The necessary requirement for plasma life is that $N_D >>> 1$ [25]:

$$N_d = \frac{4\pi}{3} n_e \lambda_D^3 \quad (6)$$

3. Materials

Aloe Vera samples were obtained from the gardens of the college of science for women. Several steps were carried out to extract and prepare the material for analysis. The process began with completely drying the Aloe Vera leaves. After that, a sample of the plant weighing 1.5 grams was ground. A press was used at a pressure of 6 Pa for ten minutes to form granules, with the diameter and thickness of the final product reaching 20 mm. The resulting material was used to study plasma spectra, and the chemical content of the sample was determined using X-ray fluorescence (XRF) analysis, which relies on analyzing the material to determine its chemical composition.

3. 1. X- Ray Fluorescence (XRF)

XRF occurs when primary X-rays (not secondary) excite the atoms in the material, leading to the emission of secondary X-rays, which are characteristic of the elements present in the material. Table 1 displays the Aloe Vera sample's (XRF) analysis. CaO has the greatest concentration value (7.762%) compared to the other elements. The interpretation of the XRF table can take into account the relationship between these elements and their role in the biological and medicinal properties of Aloe Vera. The main components found in the Aloe Vera samples were (as listed in Table 1):

CaO (calcium oxide) – 7.762%: The high calcium content indicates the role of Aloe Vera in wound healing. Calcium is essential for regulating cellular functions and also promotes tissue and cell regeneration.

Cl (chlorine) – 3.053%: Chlorine helps balance electrolytes in the plant and can contribute to its antibacterial and antifungal properties. Its role in photosynthesis also promotes the production of biologically active elements.

K_2O (potassium oxide) – 2.429%: Potassium has a significant role in maintaining the water balance in cells. In Aloe Vera, potassium may help keep the plant hydrated and enhance the moisturizing properties that Aloe Vera products are known for.

MgO (Magnesium Oxide) – 1.746%: Magnesium plays a role in chlorophyll production and enzyme activity, which may be linked to the production of antioxidants and bioactive compounds in Aloe Vera.

SO_3 (Sulfur Oxide) – 1.059%: Sulfur is important for the production of amino acids, such as cysteine and methionine, which are part of proteins and vital enzymes. The high presence of sulfur suggests that Aloe Vera can stimulate the formation of specific proteins that help treat inflammation.

P_2O_5 (Phosphorus Oxide) – 0.500%: Phosphorus is part of ATP, it provides the energy needed for the plant to manufacture active compounds, such as enzymes and antibiotics.

SiO2 (Silicon Dioxide) – 0.225%: Although silicon is not an essential nutrient, its presence enhances the plant's ability to resist environmental stress. It may play a role in supporting cellular structures and enhancing durability, which may help maintain the quality of Aloe Vera gel.

CuO (copper oxide) – 0.078%: Copper is a rare but vital element. It contributes to the production of antioxidant enzymes, which means that Aloe Vera may be effective in neutralizing free radicals that cause cell damage.

SrO (strontium oxide) – 0.051%: Although strontium has no specific function in plants, its presence in small amounts may be related to its uptake from the soil. In the medical field, strontium is used to promote bone health, and its presence in Aloe Vera may indicate potential benefits in this direction.

This distribution of elements is not only important for the mineral composition of the plant but may also indicate multiple health effects, including wound healing, moisture enhancement, and anti-oxidation. The different concentrations of the elements suggest that Aloe Vera may have overlapping therapeutic properties that could be used in medical, cosmetic, or skin care applications.

***Table 1: XRF of Aloe Vera*.**

Symbols	**Concentration**
CaO	7.762%
Cl	3.053%
K2O	2.429%
MgO	1.746%
SO_3	1.095%
$P2O_5$	0.500%
SiO_2	0.225%
CuO	0.078%
SrO	0.051%

4. Result and Discussion

The specimen's emission spectra were examined using the Nd:YAG laser, which has a wavelength of 1064 nm and a pulse repetition frequency of 10 Hz. The laser was set up with an energy range of 100 to 400 mJ and was positioned 10 cm distant from the sample. A short focal length lens results in a small beam waist (high focusing) and, consequently, can lead to high energy density and more efficient plasma generation. Light from the sample that had been subjected to a pulse laser bombardment was used by the spectrometer to perform the LIBS. The emitted light was examined using a high-speed spectrometer (Optics- HR 4000 CG-UVNIR). The light that the ablated plasma released was captured by the optical fiber, which was positioned at an angle of roughly 45 degrees. The optical fiber was placed at this angle to reduce interference between the reflected laser beam and the light emitted from the plasma. This helps improve the accuracy of the measurements, as the light emitted from the plasma is efficiently collected without interference from the original laser.

4. 1. Optical Emission Spectroscopy (OES) Analysis

The emission spectra of Aloe Vera plasma generated in the air were measured using OES at various energy levels ranging from 100 to 400 mJ. Fig. 1 displays the Aloe Vera spectra, which include the various energies of the atoms and ions that comprise the Aloe Vera. The intensity of the peaks was observed to rise with an increase in laser energy within the spectral region of 300 to 1000 nm. This type of spectroscopy is used to determine the composition of materials quickly and non-destructively and is used in many applications, such as forensic analysis of minerals and rocks. This form provides detailed information about the chemical elements present in a sample based on their spectral emissions. It can be used to compare the chemical composition between different samples or to measure the concentrations of elements in a particular sample. LIBS is used to analyze the chemical composition of materials by shining high-energy laser pulses on the sample, causing a small portion of it to vaporize and form a plasma. The plasma emits a distinctive light that can be analyzed to obtain information about the chemical elements present in the sample. The colored curves represent the spectra resulting from the different laser energies (100mJ, 200mJ, 300mJ, 400mJ). It can be seen that increasing the laser energy leads to an increase in the intensity of the spectral signal. Labelled spectral lines indicate the locations of the characteristic spectra of different elements such as calcium (Ca I, Ca II), silicon (Si I, Si

II), magnesium (MgI), potassium (KI), and chlorine (ClI). Each spectral peak in this figure is associated with a specific chemical element, and the peaks are found at specific wavelengths that reflect the electronic transitions within the atoms of these elements. As the laser energy increased, the ionization of the elements in the sample increased, leading to an increase in the intensity of the spectrum, which can be observed by the increasing height of the peaks at higher laser energies.

The equipped line slope is represented by the (-1/T), where R^2 is the statistical coefficient. It shows linear suitability efficiency, with values ranging from 0 to 1. R^2 is computed for every composition line in the shape. The best R^2 value is closer to 1, as seen in Table 2 and Fig. 2. The Excel application was used to plot this figure and calculate the y equation. The impact of biological substances in Aloe Vera, which contains complex chemical molecules such sugars, enzymes, amino acids, and phenolic compounds, is indicated by the low R^2 values shown in Table 2. When exposed to plasma, these compounds behave differently than simple or inorganic materials. Nonlinear changes in the spectrum emissions may result from these interactions. This could account for the poor coefficient of determination readings.

Table 2: Energy and Statistic Coefficient (R^2).

Energy (mJ)	R^2
100	0.323
200	0.2582
300	0.2351
400	0.2429

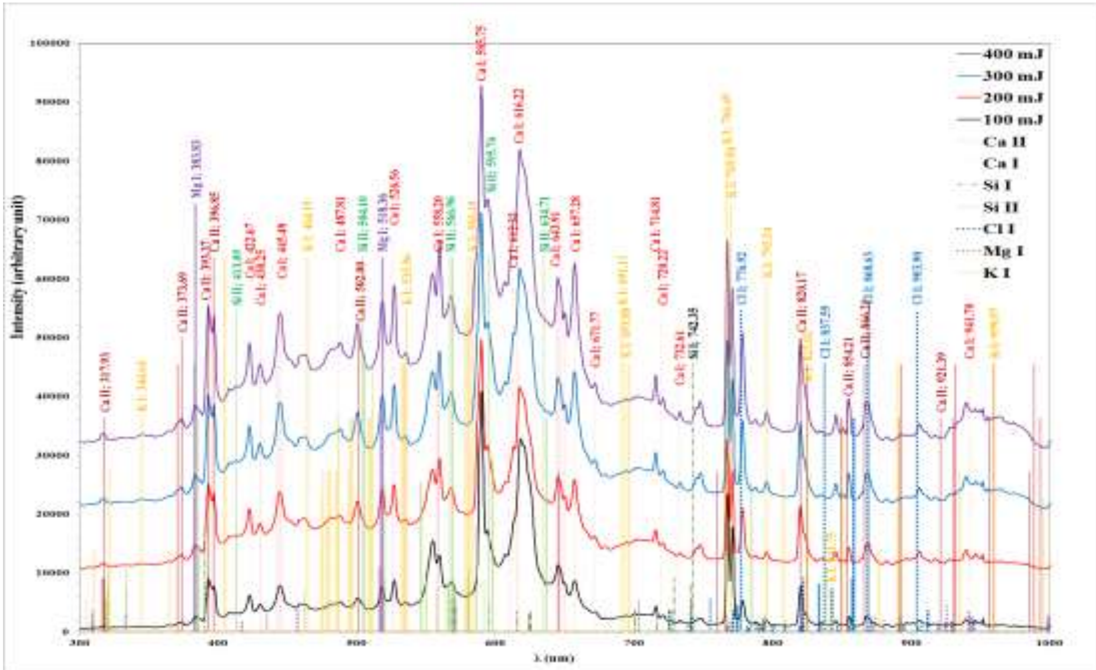

Figure 1: Aloe Vera sample plasma optical emission spectra generated in the atmosphere with varying laser power.

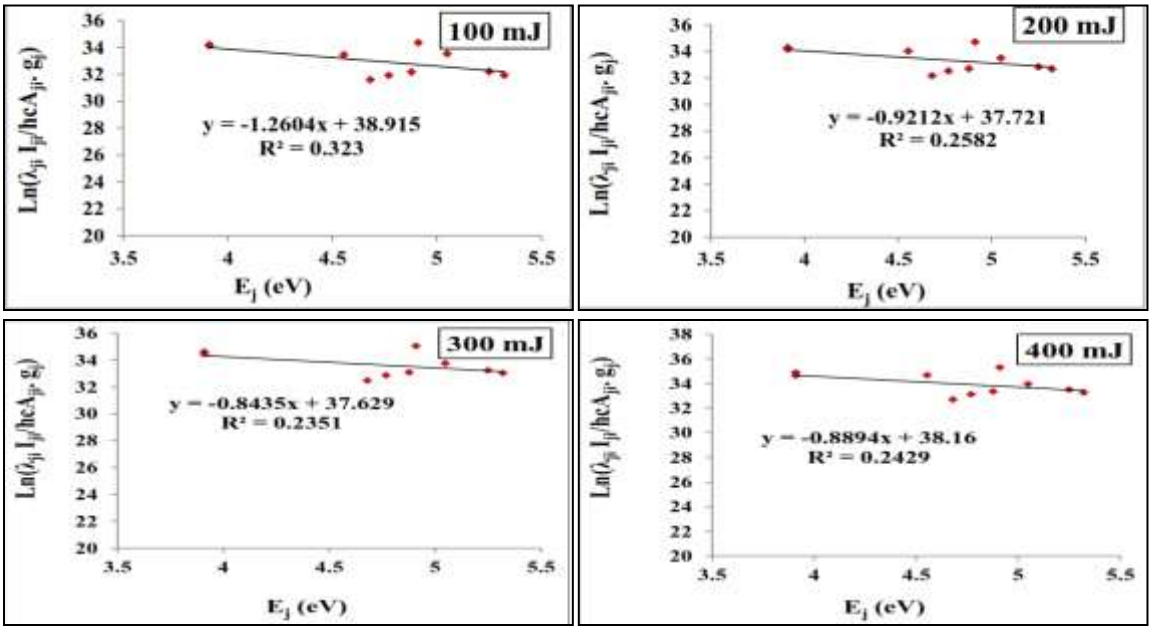

Figure 2: **Optical emission spectra for aole vera plasma produced in the air with different laser energy.**

Fig. 3 shows the Aloe Vera's striking distribution under various energies the horizontal axis of the graph shows the distribution of wavelengths (λ) of the emitted light. The vertical axis shows the intensity of the emitted light in arbitrary units. Each curve represents the intensity of the emitted light at a specific energy (100, 200, 300, and 400 mJ). It can be noted from these graphs that as the energy increased from 100 mJ to 400 mJ, the intensity of the emitted light increased, which is expected because increasing the energy leads to more excitation of the electrons, resulting in more intense emission of light. The emission peaks appeared at specific wavelengths for each energy, which can indicate the nature of the material being examined or the type of electronic transitions that occur. The dashed line represents a Lorentzian fitting of the data, which is commonly used to model spectral lines resulting from emissions or absorptions in spectroscopy. A good fit between the curve and the points can indicate that these emissions follow a typical behavior that can be described by a Lorentzian structure. Simply put, the figure shows how energy affects the intensity and wavelength of the light emission of a given material.

Fig. 4. shows that the electron temperature (T_e) and density (n_e) in the air increased as the energy increased. These data were obtained using the Boltzmann plot equation. At high laser powers, peak energy stabilizes. It can be noted from Fig. 4. that electron density (n_e) (measured in units of cm^{-3}) showed a continuous increase with increasing laser energy. When laser energy is increased, more energy is provided to excite the atoms or ions in the target material, which leads to the production of a larger number of free electrons, thus increasing the electron density. Also, electron temperature (measured in units of eV) showed an increase up to a certain limit of laser energy (of about 300 mJ), after which it began to decrease. Initially, with increasing laser energy, the kinetic energy of the electrons increases and thus their temperature increases. At a certain point, despite the increase in laser energy, the electron temperature stabilizes or even slightly decreases. This may be due to energy transfer to other processes (such as further ionization of the material rather than increasing the energy of the electrons) or due to cooling of the electrons through interactions with the surrounding environment.

The continuous increase in electron density with laser power is attributed to the increase in ionization, while the change in electron temperature reflects the complexity of the interactions occurring in the laser-generated plasma. Fig. 5 shows that Debye (λ_D) duration grew as a result of the increased energy, plasma frequency (f_p) and Debye number (N_D) growth in response to increasing laser intensity. Fig. 5 (a) expresses that increasing the laser energy led to an increase in the number of ionized or excited atoms or molecules until it reached a certain saturation. After this limit, increasing the energy did not significantly increase the number of excited atoms. Fig. 5 (b) expresses that the optical absorption coefficient increased with increasing laser energy due to increased ionization or excitation. Still, after reaching a certain value, this phenomenon began to decline due to saturation or secondary interactions. Fig. 5 (c) shows that increasing the laser energy led to a linear increase in the vibrational frequency of the material, indicating that the additional energy is mainly stored in the vibrational energy.

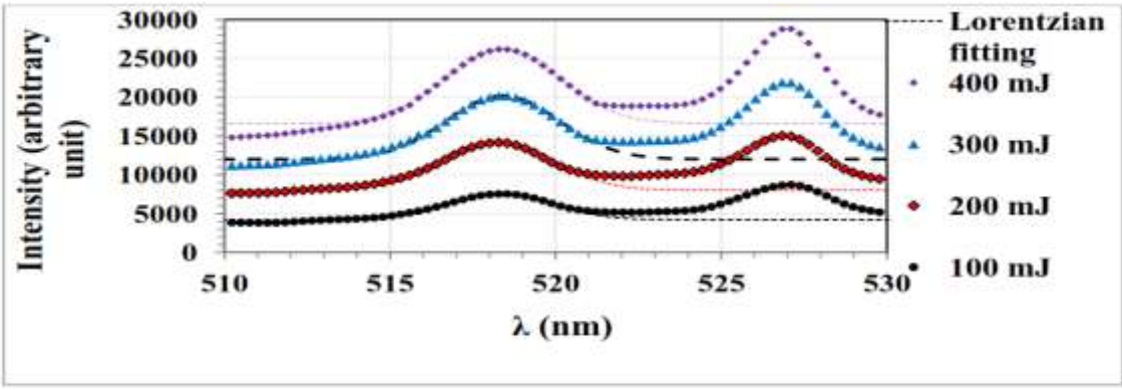

***Figure 3:** The Aloe Vera target's striking distribution at various laser energy.*

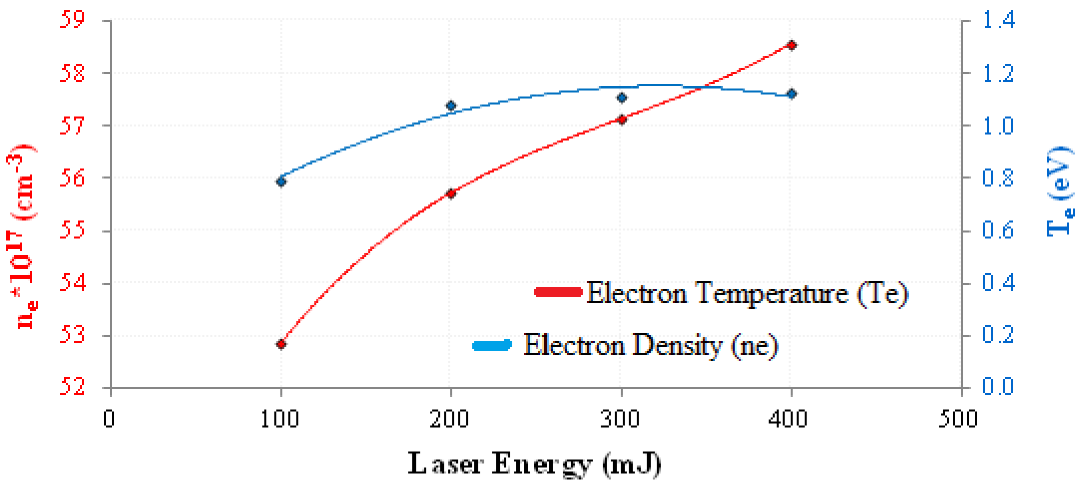

***Figure 4:** The relation between the Aloe Vera target's laser energy with T_e and n_e.*

The plasma parameter at (100–400 mJ) are displayed in Table 3. The following points can be noted:

1-Laser Energy: The laser energy directly affects how hot the resulting plasma is. As laser energy increases, more energy is transferred to the electrons and ions in the plasma, increasing the temperature of the electrons and resulting in a higher electron density.

2-Electron Temperature: The higher the laser energy, the more energy is transferred to the electrons, resulting in a higher temperature of the electrons. This means that the electrons in the plasma move at higher speeds and gain more thermal energy.

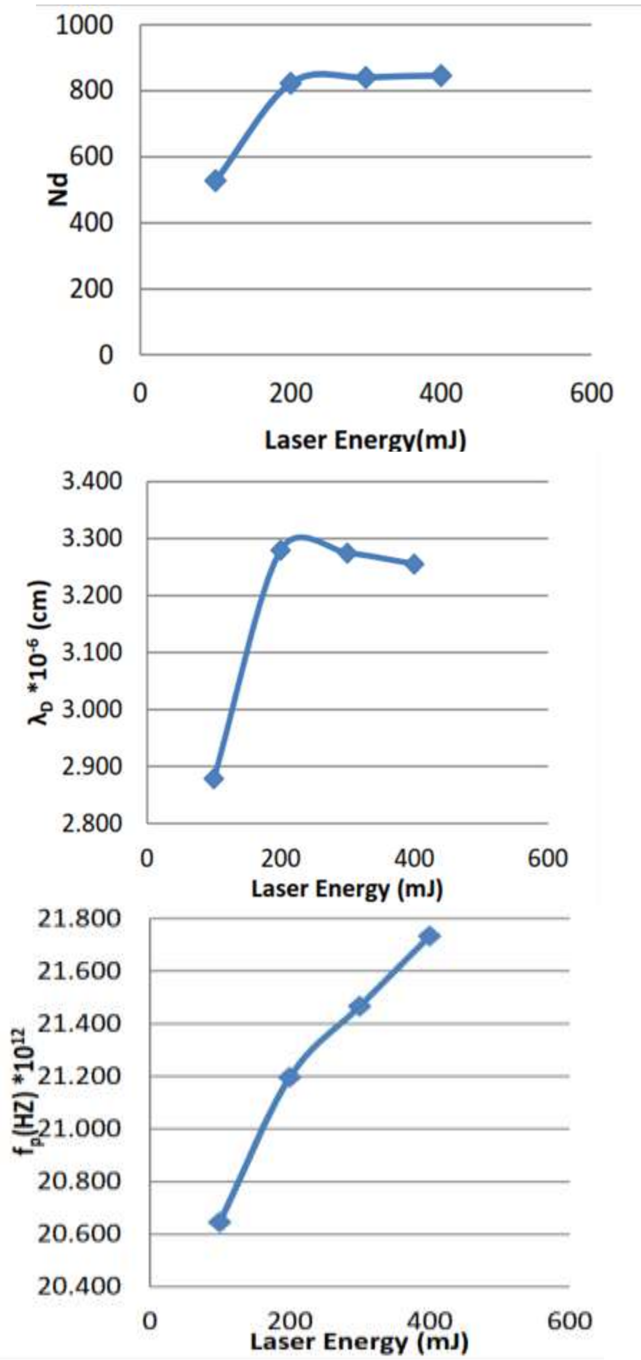

Figure 5: (a) Debye number (b) Debye length, (c) plasma frequency as a function of laser energy

3-Bandwidth (FWHM): The bandwidth reflects the spread of the spectrum produced by the laser pulse. Increasing laser energy increases the width of this spectrum, indicating more active interactions between the laser and the plasma, including ionization and excitation of electrons.

4-Electron Density (ne): The electron density represents the number of electrons per unit volume of the plasma. As laser energy increases, ionization (conversion of atoms into ions and electrons) increases, resulting in an increase in electron density.

5-Plasma Frequency (fp): The frequency of the plasma depends on the electron density. As the electron density increases due to increasing laser power, the plasma frequency increases slightly. The plasma frequency is important because it determines how the plasma interacts with electric and magnetic fields.

6-Debye length (λ_D): The Debye length is a measure of the distance at which charges in a plasma can interact with each other. Despite increasing laser power, the Debye length remains approximately constant, meaning that the effects of charges in the plasma do not change significantly as laser power increases.

7- Debye number (N_D): This value reflects the total number of particles in a given volume of plasma. As the laser power increases, the number of particles increases, indicating that the plasma has become denser and contains more charged particles.

General explanation: When high-energy laser pulses are directed at a material, the material absorbs energy, generating plasma—the fourth state of matter consisting of free electrons and ions. Increasing the laser power increases the thermal energy of the electrons and increasing their mobility. Also, the electron density increases due to the increase of ionization of the atoms in the plasma. Due to the increased electron density, the plasma frequency increased. The increase of the bandwidth indicates increased laser-matter interaction and plasma formation. These changes have a significant impact on how the plasma behaves in various applications, such as laser nuclear fusion reactions, industrial applications, and scientific research.

Table 3: The Aloe Vera Plasma parameters.

Laser energy (mJ)	T_e (eV)	FWHM (nm)	$n_e(cm^{-3})\ 10^{17}$	f_p (Hz) $*10^{12}$	λ_D (cm) $\times10^{-6}$	N_D
100	0.793	3.700	52.857	20.646	2.879	528
200	1.086	3.900	55.714	21.196	3.280	823
300	1.110	4.000	57.143	21.466	3.275	841
400	1.124	4.100	58.571	21.733	3.255	846

5. Conclusions

The effect of laser intensity on Aloe Vera spectroscopy was investigated in this study. Electron temperature and density, optical emission spectra, and other fundamental plasma properties were shown to be strongly impacted by variations in laser intensity. For Aloe Vera plasma, with increasing laser intensity, there was a nonlinear shift in electron temperature; this fluctuation in electron temperature was caused by plasma expansion. Due to the released atom's collisions with charged particles, which resulted in the Stark line broadening, which was correlated with electron density, the spectral lines looked broader as the laser intensity grew. This broadening is due to increased electron density, which is linked to higher laser intensity and resulting plasma conditions. In contrast, it was shown that an increase in mass ablation rate led to a linear increase in electron density with laser intensity.

Conflict of interest

Authors declare that they have no conflict of interest.

References

1. A. F. Ahmed, Iraqi J. Phys. **17**, 103 (2019). DOI: 10.30723/ijp.v17i42.438.
2. F. Vestin, M. Randelius, and A. Bengtson, Spectrochim. Acta Part B Atom. Spect. **65**, 721 (2010). DOI: 10.1016/j.sab.2010.04.007.
3. S. R. Mohammed, K. A. Aadim, A. H. Ali, and N. K. Abdalameer, AIP Conf. Proce. **2475**, 090009 (2023). DOI: 10.1063/5.0111674.
4. A. S. Noori, N. K. Abdalameer, S. N. Mazhir, and M. K. A. Mohammed, Int. J. Mod. Phys. B **37**, 2350100 (2022). DOI: 10.1142/S021797922350100X.
5. L. Bacakova, M. Vandrovcova, I. Kopova, and I. Jirka, Biomater. Sci. **6**, 974 (2018). DOI: 10.1039/C8BM00028J.

6. M. L. Najarian and R. C. Chinni, J. Chem. Educ. **90**, 244 (2013). DOI: 10.1021/ed3003385.
7. S. N. Mazhir, M. K. Khalaf, S. K. Taha, and H. K . Mohsin, Int. J. Eng. Tech. **7**, 1177 (2018). DOI: 10.14419/ijet.v7i3.9459.
8. H. Yuan, A. B. Gojani, I. B. Gornushkin, and X. Wang, Spectrochim. Acta Part B Atom. Spect. **150**, 33 (2018). DOI: 10.1016/j.sab.2018.10.005.
9. S. K. Taha, S. N. Mazhir, and M. K. Khalaf, Baghdad Sci. J. **15**, 0436 (2018). DOI: 10.21123/bsj.2018.15.4.0436.
10. G. H. Jihad and K. A. Aadim, Iraqi J. Phys. **16**, 1 (2018). DOI: 10.20723/ijp.16.38.1-9.
11. S. Jamali, M. A. Khoso, M. H. Zaman, Y. Jamil, W. A. Bhutto, A. Abbas, R. H. Mari, M. S. Kalhoro, and N. M. Shaikh, Phys. B Cond. Matt. **620**, 413278 (2021). DOI: 10.1016/j.physb.2021.413278.
12. A. F. Ahmed, F. a. H. Mutlak, and Q. A. Abbas, Appl. Phys. A **128**, 147 (2022). DOI: 10.1007/s00339-021-05252-8.
13. A. Iftikhar, Y. Jamil, N. Nazeer, M. S. Tahir, and N. Amin, J. Supercond. Nov. Magn. **34**, 1849 (2021). DOI: 10.1007/s10948-020-05734-5.
14. N. F. Majeed, M. R. Naeemah, A. H. Ali, and S. N. Mazhir, Iraqi J. Sci. **62**, 2565 (2021). DOI: 10.24996/ijs.2021.62.8.9.
15. M. J. Ketan and K. A. Aadim, Iraqi J. Sci. **64**, 188 (2023). DOI: 10.24996/ijs.2023.64.1.19.
16. S. N. Mazhir, ARPN J. Eng. Appl. Sci. **13**, 864 (2006).
17. U. H. Tawfeeq, A. K. Abbas, and K. A. Aadim, J. Phys.: Conf. Ser. **2114**, 012049 (2021). DOI: 10.1088/1742-6596/2114/1/012049.
18. A. H. Ali, Z. H. Shakir, A. N. Mazher, and S. N. Mazhir, Baghdad Sci. J. **19**, 0855 (2022). DOI: 10.21123/bsj.2022.19.4.0855.
19. H. M. Abdullah and A. H. Ali, Iraqi J. Phys. **21**, 58 (2023). DOI: 10.30723/ijp.v21i1.1083
20. R. Zaplotnik, G. Primc, and A. Vesel, Appl. Sci. **11**, 2275 (2021). DOI: 10.3390/app11052275.
21. S. N. Mazhir, S. K. Taha, N. H. Harb, and M. K. Khalaf, IOP Conf. Ser.: Mater. Sci. Eng. **871**, 012081 (2020). DOI: 10.1088/1757-899X/871/1/012081.
22. L. Rachdi, V. Sushkov, and M. Hofmann, Spectrochim. Acta Part B Atom. Spect. **194**, 106432 (2022). DOI: 10.1016/j.sab.2022.106432.
23. H. Mishra, M. Tichý, and P. Kudrna, Vacuum **205**, 111413 (2022). DOI: 10.1016/j.vacuum.2022.111413.
24. N. Giannakaris, G. Gürtler, T. Stehrer, M. Mair, and J. D. Pedarnig, Spectrochim. Acta Part B Atom. Spect. **207**, 106736 (2023). DOI: 10.1016/j.sab.2023.106736.
25. H. Arshad, M. Saleem, U. Pasha, and S. Sadaf, Elect. J. Biotech. **55**, 55 (2022). DOI: 10.1016/j.ejbt.2021.11.003.

تحليل معلمات البلازما لصبار الاولیفیرا باستخدام التحليل الطيفي للانبعاث البصري

وئام عقيل كاظم[1] وعلياء حسين علي[1]

[1]قسم الفيزياء، كلية العلوم للبنات، جامعة بغداد، العراق

الخلاصة

تم فحص الخصائص الرئيسية لبلازما الصبار، والتي يتم إنتاجها بواسطة نفاثة البلازما، باستخدام مطيافية الانبعاث الضوئي (OES). ومن بين خصائص البلازما التي يتم قياسها درجة حرارة الإلكترون (T_e)، وكثافة الإلكترون (n_e)، وتردد البلازما (fp)، وطول ديباي (λ_D)، ورقم ديباي (N_D). يعتمد البحث على استخدام طاقات ليزرمختلفة تتراوح من 100 إلى 400 مللي جول. تم استخدام مخطط بولتزمان الذي يعتمد على فحص شدة طيف الانبعاثات الضوئية من البلازما لحساب درجة حرارة الإلكترون. تم استخدام توسيع خط ستارك الذي يصور تأثير المجالات الكهربائية التي تنتجها الإلكترونات في البلازما على عرض الخطوط الطيفية لحساب كثافة الإلكترون. تم تعريض الهدف في هذه التجربة، مادة الصبار، لليزر على مسافة 8 سم وتم استخدام الألياف الضوئية الموضوعة على بعد 0.5 سم من الهدف لقياس الإشعاع المنبعث. وجد أن درجة حرارة الإلكترون المقاسة في الهواء تتراوح بين 0.793 و1.124 إلكترون فولت لجميع القياسات. وأظهرت النتائج أنه مع زيادة طاقة الليزر زادت درجة حرارة الإلكترون وكثافة الإلكترون. ومن المتوقع حدوث هذا الارتفاع لأن زيادة طاقة الليزر يتسبب في زيادة كمية الإلكترونات المنتجة في البلازما، مما يرفع درجة حرارة البلازما وكثافتها.

الكلمات المفتاحية: معادلة بولتزمان، توسيع خط ستارك، التحليل الطيفي للانهيار المستحث بالليزر (LIBS)، الطيف الضوئي الانبعاثي (OES)، صبار الاوليفيرا.